Enantioselective Luminescence Quenching of DNA Light-Switch [Ru(phen) 2 dppz] 2+ by Electron Transfer to Structural Homologue [Ru(phendione) 2 dppz] 2+

ARTICLE *in* THE JOURNAL OF PHYSICAL CHEMISTRY B · OCTOBER 2005

Impact Factor: 3.3 · DOI: 10.1021/jp0517091 · Source: PubMed

Enantioselective Luminescence Quenching of DNA Light-Switch $[Ru(phen)_2dppz]^{2+}$ by Electron Transfer to Structural Homologue $[Ru(phendione)_2dppz]^{2+}$

Fredrik Westerlund,* Frédéric Pierard,† Mattias P. Eng, Bengt Nordén, and Per Lincoln

Department of Chemistry and Bioscience, Chalmers University of Technology, SE−41296 Gothenburg, Sweden

Received: April 4, 2005; In Final Form: June 27, 2005

The quenching of the luminescence of $[Ru(phen)_2dppz]^{2+}$ by structural homologue $[Ru(phendione)_2dppz]^{2+}$, when both complexes are bound to DNA, has been studied for all four combinations of Δ and Λ enantiomers. Flow linear dichroism spectroscopy (LD) indicates similar binding geometries for all the four compounds, with the dppz ligand fully intercalated between the DNA base pairs. A difference in the LD spectrum observed for the lowest-energy MLCT transition suggests that a transition, potentially related to the final localization of the excited electron to the dppz ligand in $[Ru(phen)_2dppz]^{2+}$, is overlaid by an orthogonally polarized transition in $[Ru(phendione)_2dppz]^{2+}$. This would be consistent with a low-lying LUMO of the phendione moiety of $[Ru(phendione)_2dppz]^{2+}$ that can accept the excited electron from $[Ru(phen)_2dppz]^{2+}$, thereby quenching the emission of the latter. The lifetime of excited Δ-$[Ru(phen)_2dppz]^{2+}$ is decreased moderately, from 664 to 427 ns, when bound simultaneously with the phendione complex to DNA. The 108 ns lifetime of opposite enantiomer, Λ-$[Ru(phen)_2dppz]^{2+}$, is only shortened to 94 ns. These results are consistent with an average rate constant for electron transfer of approximately $1\cdot10^6$ s^{-1} between the phenanthroline− and phendione−ruthenium complexes. At binding ratios close to saturation of DNA, the total emission of the two enantiomers is lowered equally much, but for the Λ enantiomer, this is not paralleled by a decrease in luminescence lifetime. A binding isotherm simulation based on a generalized McGhee−von Hippel approach shows that the Δ enantiomer binds approximately 3 times stronger to DNA both for $[Ru(phendione)_2dppz]^{2+}$ and $[Ru(phen)_2dppz]^{2+}$. This explains the similar decrease in total emission, without the parallel decrease in lifetime for the Λ enantiomer. The simulation also does not indicate any significant binding cooperativity, in contrast to the case when Δ-$[Rh(phi)_2bipy]^{3+}$ is used as quencher. The very slow electron transfer from $[Ru(phen)_2dppz]^{2+}$ to $[Ru(phendione)_2dppz]^{2+}$, compared to the case when $[Rh(phi)_2phen]^{3+}$ is the acceptor, can be explained by a much smaller driving free-energy difference.

Introduction

Ruthenium complexes that bind noncovalently to DNA have been of great interest for the last 25 years, as this class of molecules has potential as DNA-conformational probes, anticancer drugs, or initiators for electron-transfer studies on DNA. The parent compound is the symmetric complex, $[Ru(phen)_3]^{2+}$,[1−12] where the six-coordinated ruthenium(II) ion binds the three bidentate phenanthroline moieties to form a propeller-like structure, giving two possible conformations, the right-handed (Δ) and the left-handed (Λ) enantiomer. Whether the two enantiomers of $[Ru(phen)_3]^{2+}$ bind in one of the grooves or are intercalated between the DNA base pairs has been the matter of intense discussion for many years; however, most data are consistent with a model where the complexes bind by semi-intercalating one of the phenanthroline moieties between the base pairs of DNA.[12]

The DNA-binding mode is more distinct when one of the phenanthroline moieties is extended by two aromatic rings to a dipyridophenazine (dppz) ligand, i.e., $[Ru(phen)_2dppz]^{2+}$ (**1** in Figure 1), which readily intercalates between the base pairs of DNA.[13−26] The extension to a dppz unit not only results in a stronger and more distinct DNA binding, but also in a complex with more interesting photophysical properties. Hydrogen bonding to the aza-nitrogens of the dppz moiety almost completely quenches the luminescence from **1** in aqueous solution. By contrast, when the dppz moiety intercalates between the DNA bases, the aza-nitrogens are protected from the hydrogen-bonding solvent, leading to an increase in luminescence quantum yield by several orders of magnitude ($>10^4$). This large increase in luminescence quantum yield, referred to as the "light-switch" effect,[18,27] makes the compound very useful in spectroscopic DNA-binding studies.

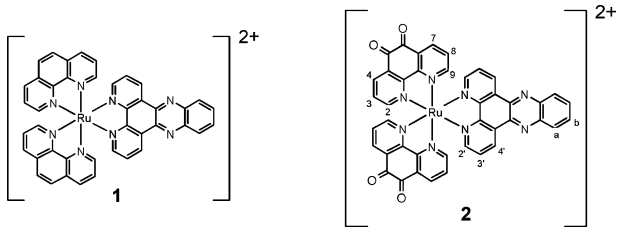

Figure 1. $[Ru(phen)_2dppz]^{2+}$ (**1**) and $[Ru(phendione)_2dppz]^{2+}$ (**2**); phen = 1,10-phenanthroline, dppz = dipyrido[3,2-a:2′,3′-c]phenazine, phendione = 1,10-phenanthroline-5,6-diketone.

When **1** is excited by light, an electron is transferred from the ruthenium(II) ion to the dppz-ligand, formally oxidizing the metal and reducing the ligand (metal-to-ligand charge transfer, MLCT). When the electron jumps back to the ruthenium(II)

* Author to whom correspondence should be addressed. Email: fredrik.westerlund@chalmers.se. Telephone: +46−31−772 30 53. Fax: +46−31−772 38 58.

† Current address: Organic Chemistry and Photochemistry, Free University of Brussels, B-1050 Brussels, Belgium.

10.1021/jp0517091 CCC: $30.25
Published on Web 08/19/2005

ion, light can be emitted, giving the complex its interesting photophysical properties. However, if the excited electron is trapped, and its energy dissipated by another process, the emission is quenched.

The rhodium complex Δ-$[Rh(phi)_2bipy]^{3+}$ (phi = phenanthrene-9,10-diimine, bipy = 2,2′-bipyridyl) quenches the luminescence of Δ-**1**, by electron transfer, with extreme efficiency, when they are both bound to DNA.[28−32] However, whether this observation is an effect of an unusually strong cooperative binding of the two complexes to DNA,[33,34] or an ultra-efficient electron transfer through the DNA base stack,[31] has been debated.

$[Ru(phendione)_2dppz]^{2+}$ (**2** in Figure 1), where the two phenanthroline moieties on **1** have been oxidized to phendiones, is nonluminescent, presumably because of a low-lying electronic state on the phendione moieties that trap the excited electron.[35−38] It would, therefore, be interesting to see if **2** could accept an electron also intermolecularly, from a simultaneously DNA-bound **1** complex, and to study the importance of the chirality for any such interactions between the two complexes.

As expected, **2** is found to bind to calf thymus DNA (CT-DNA) by intercalation, but the equilibrium constant is lower compared to **1**. The quenching of the luminescence of **1** by **2** is not at all as efficient as the quenching by Δ-$[Rh(phi)_2bipy]^{3+}$. The longest lifetime of Λ-**1** (108 ns) is lowered only about 13%, whereas the longest lifetime of Δ-**1** (664 ns) is lowered about 33%. The lowering of the total emission is, however, similar for both Δ-**1** and Λ-**1** because of a lower binding constant and, thereby, larger competition from **2** for Λ-**1**.

Materials and Methods

Chemicals. All experiments were performed in aqueous buffers (10 mM NaCl, 1 mM cacodylate at pH 7.0). Calf thymus DNA (CT-DNA), obtained from Sigma, was dissolved in buffer and filtered three times through a 0.8-μm Millipore filter before use. The enantiomers of $[Ru(phen)_2dppz]Cl_2$ (**1**) were prepared as reported elsewhere.[19] Δ- and Λ-$[Ru(phendione)_3](PF_6)_2$ were obtained by oxidation of respective $[Ru(phen)_3](PF_6)_2$ optical isomers[12,39] and isolated as PF_6^- salts by using NH_4PF_6 instead of the perchlorate used in the literature method.[40] Δ- and Λ-$[Ru(phendione)_2dppz]Cl_2$ (**2**) were synthesized from respective $[Ru(phendione)_3](PF_6)_2$ enantiomers as described below.

Δ-$[Ru(phendione)_2dppz]^{2+}$ (Δ-2). A solution of 12 mg (0.11 mmol) *o*-phenylenediamine in 5.5 mL of acetic acid/H_2O 1:10 was added dropwise with stirring to a solution of 153 mg (0.15 mmol) Δ-$[Ru(phendione)_3](PF_6)_2$ in 270 mL acetic acid/H_2O/CH_3CN 1:10:2.5. After 20 min, TLC (support SiO_2, solvent CH_3CN/KNO_3 0.1 M aqueous solution 8:1) showed the reaction to be complete. The volume of the reaction mixture was reduced to 20 mL by rotary evaporation, resulting in precipitation. Addition of 5 mL of saturated KPF_6 aqueous solution completed the precipitation of the crude product, which was collected on a filter and washed successively with water, absolute ethanol, and diethyl ether and then dried. The product was purified by column chromatography on silica gel with CH_3CN/KNO_3 0.1 M aqueous solution 8:1 as eluent. The two first fractions containing small amounts of the byproducts $[Ru(dppz)_3]^{2+}$ and $[Ru(phendione)(dppz)_2]^{2+}$ were discarded; the large third fraction gave Δ-**2**. After the solvent was removed from the desired fraction, the complex was redissolved in water, isolated as the PF_6 salt by precipitation with aqueous KPF_6, and washed twice with water. An additional recrystallization from acetonitrile/diethyl ether yielded 38 mg (32%) of Δ-$[Ru(phendione)_2dppz](PF_6)_2$. Conversion to dichloride salts was achieved through anion-exchange chromatography (1:1 acetonitrile/water eluent) on Sephadex QAE−25 (Aldrich). The Λ enantiomer of **2** was prepared in the same way from Λ-$[Ru(phendione)_3](PF_6)_2$. ^{1}H NMR for Δ-**2**$(PF_6)_2$ (300 MHz, CD_3CN, 298 K, see Figure 1 for proton numbering): δ ppm = 9.74 (dd, 2H, $^3J_{3'4'}$ = 8.4 Hz, $H_{4'}$), 8.61 (d, 2H, $^3J_{34}$ = 7.8 Hz, H_4), 8.51 (d, 2H, $^3J_{78}$ = 7.8 Hz, H_7), 8.50 (dd, 2H, $^3J_{ab}$ = 6.6 Hz, H_b), 8.32 (dd, 2H, $^4J_{2'4'}$ = 1.2 Hz, $H_{2'}$), 8.22 (d, 2H, $^3J_{23}$ = 5.7 Hz, H_2), 8.16 (dd, 2H, $^4J_{ab}$ = 3.6 Hz, H_a), 8.00 (d, 2H, H_9), 7.96 (dd, 2H, $^3J_{2'3'}$ = 5.4 Hz, $H_{3'}$), 7.72 (dd, 2H, H_3), 7.52 (dd, 2H, $^3J_{89}$ = 5.7 Hz, H_8). ES-MS for Δ-**2**$(PF_6)_2$ (acetonitrile/water 1:1): *m*/*e* = 402.2 (100%, calcd $[M\text{-}2PF_6^-]^{2+}$ = 402.0), 411.3 (100%, calcd $[M\text{-}2PF_6^- + H_2O]^{2+}$ = 411.0), 420.2 (68%, calcd $[M\text{-}2PF_6^- + 2H_2O]^{2+}$ = 420.0), 429.2 (10%, calcd $[M\text{-}2PF_6^- + 3H_2O]^{2+}$ = 429.0). Hydration of the carbonyl groups in 1,10-phenanthroline-5,6-dione coordinated to metal cations has been previously reported in the literature.[41−43] UV−vis for Δ-**2**$(Cl)_2$ [water, λ_{max}/nm, (ϵ/1000 M^{-1} cm^{-1})]: 432 (16.0), 372 (15.4, shoulder), 355 (17.5), 292 (57.1, shoulder), 278 (62.5). CD for Δ-**2**$(Cl)_2$ [water, λ_{extr}/nm, ($\Delta\epsilon$/M^{-1} cm^{-1})]: 482 (−11.0), 410 (+16.9), 349 (+2.0), 306 (−91.5), 298 (−77.0), 276 (−5.6), 258 (−14.5). (ee = 0.99) The CD signals for Λ-**2**$(Cl)_2$ were of the same amplitude and opposite signs (ee = 0.96). The enantiomeric excess (ee) was estimated from CD measurements in water with a sample of Δ-$[Ru(dppz)_3][Cl_2]$ prepared under similar conditions from the same starting material Δ-$[Ru(phendione)_3](PF_6)_2$ and compared to the literature value for a reference sample of Δ-$[Ru(dppz)_3][Cl_2]$.[40]

Sample Preparation. Samples were prepared by mixing equal volumes of ruthenium complex and DNA dissolved in buffer. The final sample concentrations were 10 μM of complex and 160 μM of DNA for LD measurements. Concentrations were determined on a Varian Cary 4B spectrophotometer. The extinction coefficients used were: ϵ_{440nm} = 20 000 M^{-1} cm^{-1} for $[Ru(phen)_2dppz]^{2+}$, ϵ_{432nm} = 16 000 M^{-1} cm^{-1} for $[Ru(phendione)_2dppz]^{2+}$, and ϵ_{260nm} = 6600 M^{-1} cm^{-1} for ct-DNA.

Flow Linear Dichroism. Linear dichroism (LD)[44] is defined as the difference in absorbance of linearly polarized light parallel and perpendicular to a macroscopic orientation axis (here the flow direction):

$$LD(\lambda) = A_{||}(\lambda) - A_{\perp}(\lambda)$$

Samples with ruthenium complex and DNA were oriented in a Couette flow cell with an outer rotating cylinder at a shear gradient of 3000 s^{-1}. LD spectra were measured on a Jasco J-720 CD spectropolarimeter equipped with an Oxley prism to obtain linearly polarized light. All spectra were recorded between 220 and 650 nm and baseline-corrected by subtracting the spectrum recorded for the nonoriented sample.

Steady-State Luminescence Measurements. Emission spectra were recorded on a xenon lamp equipped SPEX fluorolog τ-2 spectrofluorimeter (JY Horiba) between 420 and 800 nm using an excitation wavelength of 415 nm. Using a short optical path length for the excitation light, the inner filter effect due to excitation light absorption was kept below 10%.

Transient Emission Measurements. The nanosecond emission decay measurements were performed on a setup where the exciting light is provided by a pulsed Nd:YAG laser (Continuum Surelite II-10, pulse width <7 ns) pumping an optical parametric oscillator (OPO), giving a tunable excitation wavelength between 400 and 700 nm. The emitted light was collected at an angle of 90° relative to the excitation light and, after passing a monochromator (symmetrical Czerny−Turner arrangement),

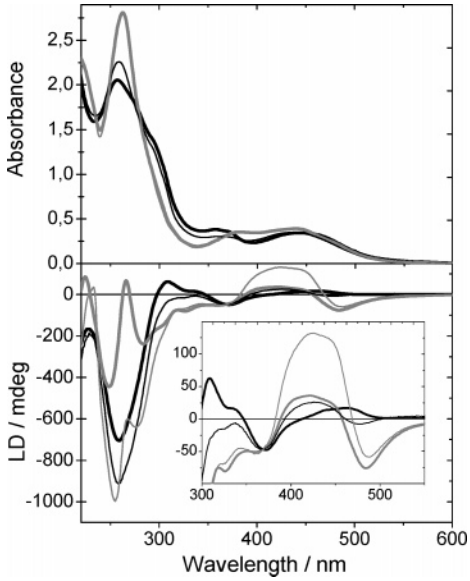

Figure 2. Absorbance spectra (top) and LD spectra (bottom) of **Δ-1** (thick gray line), **Λ-1** (thin gray line), **Δ-2** (thick black line) and **Λ-2** (thin black line), bound to CT-DNA at a P/Ru ratio of 8. Inset shows the LD spectra zoomed between 300 and 550 nm. Measurements performed at 25 °C in 10 mM NaCl, 1 mM cacodylate buffer, pH 7.

detected by a five-stage Hamamatsu R928 photomultiplier tube. The decays were collected and averaged by a 200 MHz digital Oscilloscope (Tektronix TDS2200 2Gs/s) and stored by a LabView program (developed at the department), which controls the whole instrument setup. The oscilloscope is triggered by a photodiode that detects the exciting laser pulse.

In the experiments, an excitation wavelength of 440 nm was used, and the emission decays were probed at 620 nm. In general, 16 decays were collected and averaged for each sample. The energy of the exciting laser was kept below 20 mJ/pulse to prevent photodegradation of the samples.

Mathematical Simulations. The theory method used in the mathematical simulation of the binding isotherms is based on interactions between neighboring molecules only, treating DNA as a linear lattice with identical binding sites. The model used is a generalized version of the probabilistic approach of McGhee and von Hippel.[33,34,45] The simulations were performed in MatLab.

Results & Discussion

Binding Studies of [Ru(phendione)$_2$dppz]$^{2+}$ to DNA. The DNA-binding mode of [Ru(phendione)$_2$dppz]$^{2+}$ (**2**), was characterized by flow linear dichroism (LD) measurements. Figure 2 shows the absorption spectra (top) and the LD spectra (bottom) of each of the two enantiomers of **2** bound to CT-DNA, compared with those of **1**, with a Ru complex-to-base-pair ratio of 1:4. Figure 3 shows LD spectra for corresponding titration series for the two enantiomers of **2** as well as the two enantiomers of **1**. The LD spectra may be interpreted in terms of binding geometry on the basis of the transition moment directions, the major three MLCT moments shown in Figure 4, as has been earlier assigned for **1**.[21] The amplitude of the negative LD peak at 370 nm in relation to the isotropic absorbance indicates that the in-ligand $\pi-\pi^*$ transition of the dppz moiety is perpendicular to the DNA helix axis, consistent with intercalation.[19,21]

From the similar LD spectral behavior of **2**, we conclude that also this compound is intercalated. The origin of the conspicuously different LD spectra in the region 400−500 nm of the

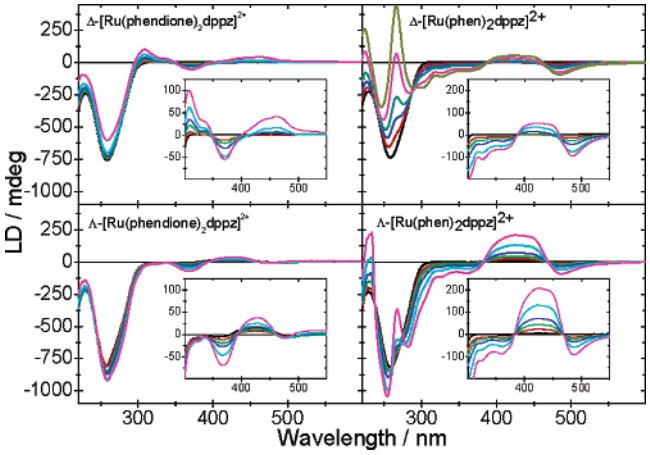

Figure 3. LD spectra of **Δ-2** (top left), **Λ-2** (bottom left), **Δ-1** (top right) and **Λ-1** (bottom right) bound to CT-DNA at different binding ratios (P/Ru values of 50 (red), 25 (green), 15 (blue), 8 (cyan) and 4 (magenta)). The signal increases with increasing amount of complex. Black curve is pure CT-DNA at the same concentration as in all other measurements. Insets show an enlargement of the LD spectra between 300 and 550 nm. Note the different *y*-axis scale for the insets. The insets for **2** are zoomed in twice as much as the ones for **1**. Measurements performed at 25 °C in 10 mM NaCl, 1 mM cacodylate buffer, pH 7.

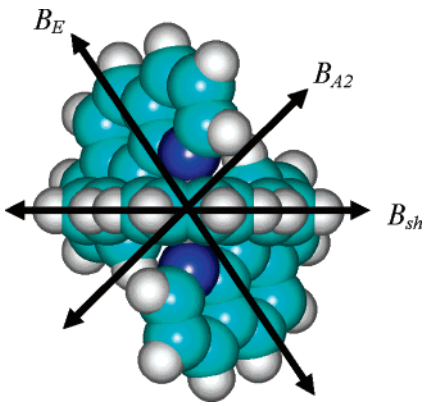

Figure 4. The three major *B* polarized transition moment polarizations of [Ru(phen)$_2$dppz]$^{2+}$, depicted for the Δ enantiomer, oriented with the 2-fold axis perpendicular to the plane of the paper. In addition, there are two important transitions with A symmetry, polarized perpendicular to the plane of the paper, viz. the in-ligand long-axis polarized $\pi-\pi^*$ transition of dppz at ca. 370 nm and the MLCT transition responsible for the negative LD band at ca. 480 nm for **1**, but not visible for **2**.

two enantiomers of **1** bound to CT-DNA is well understood: it is due to a small roll around the 2-fold axis of the complex away from an idealized all-perpendicular intercalation geometry, interestingly, by about the same angle and the same direction (clockwise) for opposite enantiomers.[21] A clockwise rotation around the 2-fold axis by 10−20° is consistent with a conformational change to A-form DNA, provided that the complex is inserted from the minor groove (an anticlockwise rotation be expected for binding from the major groove). We see a qualitatively similar spectral behavior with **2** and conclude that the enantiomers bind with binding geometries that are grossly similar to those earlier reported for **1**, i.e., that the dppz moiety is intercalating between base pairs of DNA. The change in the LD amplitude for the DNA base absorption at 260 nm when the ruthenium complexes bind indicates that the trend of a somewhat improved DNA orientation for the **Λ** enantiomer and

somewhat decreased DNA orientation for the Δ enantiomer, earlier observed for homomorphous Ru oligopyridyl compounds, including **1**, also occurs with **2**.[12]

However, there are also noticeable differences. The magnitude of the positive B_E band at 400−450 nm is much smaller and differs less between the two enantiomers for **2** compared to **1** (the B_E polarization would come close to the magic angle 55° relative to the DNA helix axis, and hence LD = 0, for the case where there is no roll away from the standard perpendicular intercalation geometry).[19,21] A smaller average roll could indicate either that the complex does not induce the A conformation in DNA or that it may intercalate with equal probability from the minor and major grooves, so that clockwise and anticlockwise rolls cancel in the LD spectrum. Another difference is that the distinct LD peak in the UV region at 270 nm of **1** is not present for **2**. This peak is due to a B_{A2} transition from exciton coupling between the strong long-axis $\pi-\pi^*$ transitions of the phenanthroline moieties and is not expected to occur in a phendione complex. Somewhat surprisingly, though, the distinct negative LD peaks observed for both enantiomers of **1** at about 480 nm are not present at all for both Δ-**2** and Λ-**2**. Because this absorption band has the same polarization along the complex 2-fold axis (A) as the dppz band at 370 nm (Figure 4), its absence cannot be attributed to a different binding geometry but must instead be due to the different electronic structure of **2**. Because the isotropic absorption band of **2** is not significantly different from **1** in the long-wavelength MLCT absorption, the difference is assigned the result of a subtle shift of the A component toward higher energy and the E components to lower energy, because of different frontier orbitals of the phendione ligands, so that its negative LD is swamped by the positive LD of the higher energy MLCT bands, thereby increasing the mutual cancellation of the A and E transitions in the LD spectrum.[21]

The luminescence quantum yield is much lower for **2** than for **1** when bound to CT-DNA, only about 2% of that of Λ-**1**, probably because of the possibility of the phendione moieties to trap the excited electron in a nonluminescent excited state. From symmetry, and on the basis of the polarization evidence from LD above, it may be argued that the LUMO MLCT state in **1** be dominated by antibonding π-orbitals (with A symmetry) localized on the dppz ligand, which explains the pronounced light switch effect, whereas in **2**, the subtle energy shift of this state to higher energy leads to a preferential localization of the electron to the phendione ligands.

Quenching. Samples of both enantiomers of **1** bound to DNA were titrated with each enantiomer of **2**, and emission spectra were recorded. Figure 5 shows the decrease in integrated emission intensity with increasing concentration of **2**. For each combination of complexes, three different binding ratios of **1** to DNA were investigated.

The quenching of **1** is expected to increase with a decreasing number of available binding sites because that will bring **1** and **2** statistically closer together and will also increase the competition between **1** and **2** for available binding sites. The effect of dissociation should be negligible when **1** is bound at higher P/**1** ratios; however, quenching is also observed at these ratios with Δ-**1**. It is noticeable that the differences in quenching efficiency are much larger when changing the chirality of the molecule that is quenched (**1**) than when changing the chirality of the quencher (**2**). It should be kept in mind that the emission quantum yield for **1** changes with the DNA binding density; however, the quantum yield increases when the binding density is increased, opposite to the decrease in emission observed here.[19,22]

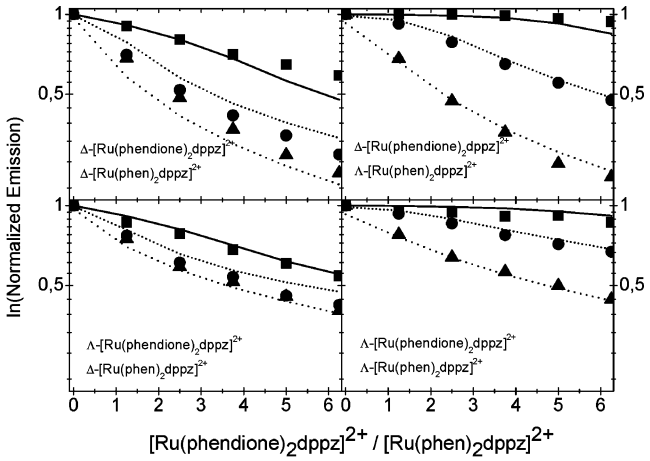

Figure 5. Relative decrease in emission from Δ-**1** and Λ-**1** with increasing concentration of Δ-**2** and Λ-**2**, respectively. Experimental results shown as scatter, and simulated data shown as lines. The P/**1** ratios are 16 (squares, solid line), 8 (circles, dashed line), and 4 (triangles, dotted line). The concentration of **1** is kept at 3 μM, and the DNA concentration is varied accordingly. The *x*-axis values are ratios between the amount of added **2** and **1**. Measurements performed at 25 °C in 10 mM NaCl, 1 mM cacodylate buffer, pH 7. The parameters used for the simulations are $K_{\Delta-1} = 10 \times 10^6$ M^{-1}, $K_{\Lambda-1} = 3.5 \times 10^6$ M^{-1}, $K_{\Delta-2} = 2.8 \times 10^6$ M^{-1}, $K_{\Lambda-2} = 1.0 \times 10^6$ M^{-1} for the binding constants and $n = 2.3$ for the size of the binding sites for all four enantiomers.

TABLE 1: Luminescence Lifetimes of Δ-1 and Λ-1 Bound to DNA with Increasing Concentration of Λ-2

3 μM Δ-**1** + *X* μM Λ-**2**	τ_1/ns[a]	τ_2/ns + −0.5 ns
X = 0	664 (0.38)	89 (0.62)
3	588 (0.35)	69 (0.65)
6	507 (0.32)	58 (0.68)
9	473 (0.30)	52 (0.70)
12	452 (0.28)	48 (0.72)
15	427 (0.26)	41 (0.74)
3 μM Λ-**1** + *X* μM Λ-**2**	τ_1/ns + −1 ns	τ_2/ns + −0.25 ns
X = 0	108 (0.39)	23 (0.61)
3	97 (0.42)	18 (0.58)
6	94 (0.43)	17 (0.57)
9	96 (0.42)	16 (0.58)
12	96 (0.41)	15 (0.59)
15	94 (0.41)	15 (0.59)

[a] Excited-state lifetimes (τ), and in parentheses, normalized pre-exponential factors reflecting mole fractions of the different luminescent species at $t = 0$ (directly after illumination), provided the luminophore is assumed to have the same radiative decay rate in each environment. The concentration of **1** is 3 μM, and the DNA concentration is 12 μM. The concentration of **2** is given in the left column. Measurements performed at 25 °C in 10 mM NaCl, 1 mM cacodylate buffer, pH 7. Standard deviations for the lifetimes are approximately 5−10%.

To study these processes further, we also measured the luminescence lifetimes by time-resolved emission studies. As can be seen in Table 1, both the luminescence lifetimes for Δ-**1** are quenched significantly, while the luminescence lifetimes for Λ-**1** are much less affected.

Figure 6 shows a comparison of the total integrated emission and the sum $\sum (\alpha_i \tau_i)$ for Λ-**1** and Δ-**1**, respectively. The surprising observation is that, even though the lifetimes of Δ-**1** are affected much more than the ones for Λ-**1**, the decrease in total integrated emission is rather similar. Assuming that the quenching rate constant is the same for Λ-**1** and Δ-**1**, the fact that the lifetimes for Δ-**1** decrease more than the ones for Λ-**1** is not surprising. Because Δ-**1** remains in the excited state for a longer time than Λ-**1**, **2** has more time to quench Δ-**1** than

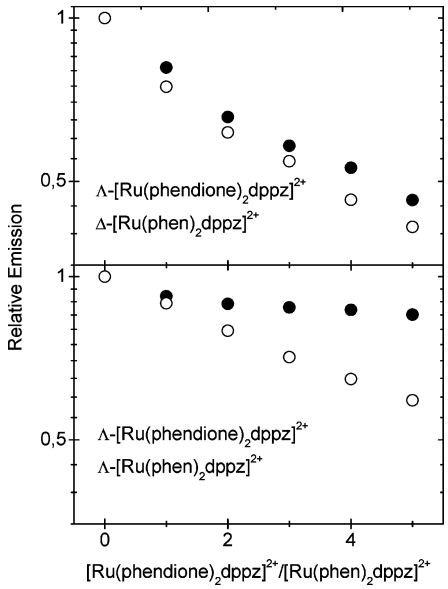

Figure 6. Comparison of the sum $\sum(\alpha_i\tau_i)$ (full circles) and the total steady-state emission (empty circles) for Δ-**1** (top panel) and Λ-**1** (bottom panel), quenched by an increasing concentration of Λ-**2**, pH 7. The concentration of **1** is 3 μM, and the DNA concentration is 12 μM. The *x*-axis values are ratios between the amount added **2** and **1**. Measurements performed at 25 °C in 10 mM NaCl, 1 mM cacodylate buffer, pH 7. Data normalized to 1 for no **2** added.

Λ-**1**. The decrease of steady-state emission observed for Λ-**1**, that reaches similar values as for Δ-**1**, can possibly be explained by a lower DNA-binding constant for Λ-**1** than for Δ-**1**, or that a fraction of bound Λ-**1** has a very short lifetime due to an efficient static quenching by **2**.

Simulations of the experimental data were performed to find out more about the binding constants and possible differences in cooperativity between **1** and **2**, depending on chirality. Figure 5 shows a good agreement between the simulations and the experimental results. In contrast to the quenching of **1** by $[Rh(phi)_2bipy]^{3+}$,[33] no cooperativity effects were needed to be taken into account when simulating the simultaneous binding of **1** and **2** to DNA. A good fit required individual values for the binding constants for the four different complexes; however, a common value on the size of the binding site ($n = 2.3$ base pairs) was sufficient. The binding constant for the Δ complex is about 3 times larger than that for the corresponding Λ complex for both **1** and **2**, and the binding constant for **1** is 4 times stronger than for **2** when the corresponding enantiomers are compared. The longer lifetime for Δ-**1** explains why bound Δ-**1** is quenched and not Λ-**1**. The decreased emission from Λ-**1** is mainly due to dissociation of Λ-**1** upon binding of **2**, whereas Δ-**1** has a decreased emission, also due to quenching, as a consequence of its longer lifetime. The lower binding constants found for **2** compared to **1** suggests that the middle ring of the phenanthroline contributes to the binding of **1** to DNA. However, whether the lower binding constant for **2** is due to decreased hydrophobic interactions or unfavorable steric or electrostatic repulsion is yet to be determined.

Because there is negligible spectral overlap between the emission of **1** and the absorbance of **2**, Förster type fluorescence resonance energy transfer (FRET) is not likely to be the primary cause of the quenching. The quenching must then be of some other kind, presumably electron transfer from **1** to the phendiones on **2**, although Dexter type triplet energy transfer cannot be excluded. However, it is spectroscopically difficult to distinguish between the two different processes because the produced charge transfer states differ only in the location of the electron hole. The striking thing is how slow the quenching is. Λ-**1** has a lifetime of 108 ns that is shortened to 94 ns and Δ-**1** is quenched from 664 to 427 ns. This means that the rate constant for electron transfer (k_{ET}) can be calculated to be between $0.8\cdot10^6$ and $1.4\cdot10^6$ s^{-1}. The equation used for calculation of k_{ET} is the definition of lifetime[46]

$$\tau = \frac{1}{k_{ET} + k}$$

(where k_{ET} is zero without quencher), giving

$$k_{ET} = \frac{1}{\tau_q} - \frac{1}{\tau_0}$$

where k_{ET} is the rate constant for electron transfer, k is the rate constant for all other processes that relaxes the excited state, τ_q is the lifetime with quencher, and τ_0 is the lifetime without quencher.

The driving force for the quenching by electron transfer from $[Ru(phen)_2dppz]^{2+}$ by $[Rh(phi)_2phen]^{3+}$ is estimated to about −0.79 eV.[28] When comparing the driving force for electron transfer from **1** to $[Rh(phi)_2phen]^{3+}$ to the driving force from **1** to **2**, only the reduction potential of the acceptor needs to be taken into account. A reduction potential of +0.02 V vs NHE is reported in the literature for $[Rh(phi)_2phen]^{3+}$ (in DMF). The reduction potential for **2** can be approximated by using the reported electrochemistry data for a phendione coordinated to a ruthenium(II) ion, as in $[Ru(phen)_2phendione]^{2+}$. This complex has a redox potential of −0.51 V vs SCE[35] in acetonitrile (equals −0.75 V vs NHE). There is thus a much smaller driving force (−0.02 V) for electron transfer from **1** to **2** than to $[Rh(phi)_2phen]^{3+}$, partly explaining the slow rate constant for electron transfer from **1** to **2**. A contributing mechanism for the inefficient electron transfer could be stabilization of the quinone ligands in aqueous solution due to formation of *gem*-diols by addition of water to the carbonyl groups.[41,42]

Acknowledgment. Frédéric Pierard is grateful to The Marie Curie Fellowship program of the EU for a research grant.

References and Notes

(1) Barton, J. K.; Danishefsky, A.; Goldberg, J. *J. Am. Chem. Soc.* **1984**, *106*, 2172−2176.
(2) Kumar, C. V.; Barton, J. K.; Turro, N. J. *J. Am. Chem. Soc.* **1985**, *107*, 5518−5523.
(3) Barton, J. K.; Goldberg, J. M.; Kumar, C. V.; Turro, N. J. *J. Am. Chem. Soc.* **1986**, *108*, 2081−2088.
(4) Pyle, A. M.; Rehmann, J. P.; Meshoyrer, R.; Kumar, C. V.; Turro, N. J.; Barton, J. K. *J. Am. Chem. Soc.* **1989**, *111*, 3051−3058.
(5) Rehmann, J. P.; Barton, J. K. *Biochemistry* **1990**, *29*, 1710−1717.
(6) Rehmann, J. P.; Barton, J. K. *Biochemistry* **1990**, *29*, 1701−1709.
(7) Eriksson, M.; Leijon, M.; Hiort, C.; Norden, B.; Graeslund, A. *J. Am. Chem. Soc.* **1992**, *114*, 4933−4934.
(8) Satyanarayana, S.; Dabrowiak, J. C.; Chaires, J. B. *Biochemistry* **1992**, *31*, 9319−9324.
(9) Satyanarayana, S.; Dabrowiak, J. C.; Chaires, J. B. *Biochemistry* **1993**, *32*, 2573−2584.
(10) Eriksson, M.; Leijon, M.; Hiort, C.; Norden, B.; Graslund, A. *Biochemistry* **1994**, *33*, 5031−5040.
(11) Nordén, B.; Lincoln, P.; Åkerman, B.; Tuite, E. *Met. Ions Biol. Syst.* **1996**, *33*, 177−252.
(12) Lincoln, P.; Nordén, B. *J. Phys. Chem. B* **1998**, *102*, 9583−9594.
(13) Balzani, V.; Ballardini, R. *Photochem. Photobiol.* **1990**, *52*, 409−416.
(14) Pyle, A. M.; Barton, J. K. *Prog. Inorg. Chem.* **1990**, *38*, 413−75.
(15) Friedman, A. E.; Kumar, C. V.; Turro, N. J.; Barton, J. K. *Nucleic Acids Res.* **1991**, *19*, 2595−2602.
(16) Hartshorn, R. M.; Barton, J. K. *J. Am. Chem. Soc.* **1992**, *114*, 5919−5925.

(17) Chow, C. S.; Barton, J. K. *Methods Enzymol.* **1992**, *212*, 219−242.

(18) Jenkins, Y.; Friedman, A. E.; Turro, N. J.; Barton, J. K. *Biochemistry* **1992**, *31*, 10809−10816.

(19) Hiort, C.; Lincoln, P.; Nordén, B. *J. Am. Chem. Soc.* **1993**, *115*, 3448−3454.

(20) Haq, I.; Lincoln, P.; Suh, D.; Nordén, B.; Chowdhry, B. Z.; Chaires, J. B. *J. Am. Chem. Soc.* **1995**, *117*, 4788−4796.

(21) Lincoln, P.; Broo, A.; Nordén, B. *J. Am. Chem. Soc.* **1996**, *118*, 2644−2653.

(22) Tuite, E.; Lincoln, P.; Nordén, B. *J. Am. Chem. Soc.* **1997**, *119*, 239−240.

(23) Holmlin, R. E.; Stemp, E. D. A.; Barton, J. K. *Inorg. Chem.* **1998**, *37*, 29−34.

(24) Nair, R. B.; Murphy, C. J. *J. Inorg. Biochem.* **1998**, *69*, 129−133.

(25) Erkkila, K. E.; Odom, D. T.; Barton, J. K. *Chem. Rev.* **1999**, *99*, 2777−2795.

(26) Olofsson, J.; Önfelt, B.; Lincoln, P. *J. Phys. Chem. A* **2004**, *108*, 4391−4398.

(27) Friedman, A. E.; Chambron, J. C.; Sauvage, J. P.; Turro, N. J.; Barton, J. K. *J. Am. Chem. Soc.* **1990**, *112*, 4960−4962.

(28) Murphy, C. J.; Arkin, M. R.; Ghatlia, N. D.; Bossmann, S.; Turro, N. J.; Barton, J. K. *Proc. Natl. Acad. Sci. U.S.A.* **1994**, *91*, 5315−5319.

(29) Murphy, C. J.; Arkin, M. R.; Jenkins, Y.; Ghatlia, N. D.; Bossmann, S. H.; Turro, N. J.; Barton, J. K. *Science* **1993**, *262*, 1025−1029.

(30) Arkin, M. R.; Stemp, E. D. A.; Turro, C.; Turro, N. J.; Barton, J. K. *J. Am. Chem. Soc.* **1996**, *118*, 2267−2274.

(31) Franklin, S. J.; Treadway, C. R.; Barton, J. K. *Inorg. Chem.* **1998**, *37*, 5198−5210.

(32) Stemp, E. D. A.; Holmlin, R. E.; Barton, J. K. *Inorg. Chim. Acta* **2000**, *297* (1−2), 88−97.

(33) Lincoln, P.; Tuite, E.; Norden, B. *J. Am. Chem. Soc.* **1997**, *119*, 1454−1455.

(34) Lincoln, P. *Chem. Phys. Lett.* **1998**, *288*, 647−656.

(35) Campagna, S.; Serroni, S.; Bodige, S.; MacDonnell, F. M. *Inorg. Chem.* **1999**, *38*, 692−701.

(36) Goulle, V.; Harriman, A.; Lehn, J.-M. *J. Chem. Soc., Chem. Commun.* **1993**, 1034−1036.

(37) Kim, M.-J.; Konduri, R.; Ye, H.; MacDonnell, F. M.; Puntoriero, F.; Serroni, S.; Campagna, S.; Holder, T.; Kinsel, G.; Rajeshwar, K. *Inorg. Chem.* **2002**, *41*, 2471−2476.

(38) Lopez, R.; Leiva, A. M.; Zuloaga, F.; Loeb, B.; Norambuena, E.; Omberg, K. M.; Schoonover, J. R.; Striplin, D. R.; Devenney, M.; Meyer, T. J. *Inorg. Chem.* **1999**, *38*, 2924−2930.

(39) Broomhead, J. A.; Young, C. G. *Inorg. Synth.* **1990**, *28*, 338−340.

(40) Torres, A. S.; Maloney, D. J.; Tate, D.; Saad, Y.; MacDonnell, F. M. *Inorg. Chim. Acta* **1999**, *293*, 37−43.

(41) Lei, Y.; Anson, F. C. *J. Am. Chem. Soc.* **1995**, *117*, 9849−9854.

(42) Lei, Y.; Shi, C.; Anson, F. C. *Inorg. Chem.* **1996**, *35*, 3044−3049.

(43) Larsson, K.; Öhrström, L. *Inorg. Chim. Acta* **2004**, *357*, 657−664.

(44) Nordén, B.; Kubista, M.; Kurucsev, T. *Q. Rev. Biophys.* **1992**, *25* (1), 51−170.

(45) McGhee, J. D.; von Hippel, P. H. *J. Mol. Biol.* **1974**, *86*, 469−89.

(46) Lakowicz, J. R. *Principles of Fluorescence Spectroscopy*; Plenum Press: New York, 1983.